3D TEXTURE MODELS FOR IMAGES OF 3D SCENES

Fernand S. Cohen and Maqbool A. Patel

Electrical and Computer Engineering Department
Drexel University
Philadelphia, PA 19104, USA

Abstract

This paper presents a *novel* and *computationally efficient* way of modelling images that result from the projective distortions of homogeneous textures laid on illuminated 3D surfaces, as they are seen by a camera. We use a "homogeneous" Gaussian Markov Random Field (GMRF) for modelling the texture. The GMRF has been shown to faithfully reproduce a vast class of micro and macro planar "homogeneous" image textures. To transform the GMRF's into 3D texture models, we reflect in the GMRF probability distribution function, the functional relationships that exist between the image of a homogeneous textured plane when viewed head-on by a camera (with either "orthographic" or "perspective" geometry), and the image produced by the same plane when it is given an orientation relative to the optical-axis of the camera. The resulting 3D texture model is a GMRF whose parameters are the texture characteristics and the surface shape, and the camera model. The model is synthesizable, and hence one can visually judge its goodness in capturing the projective distortions (seen by a camera) of a texture laid on an illuminated surface. It is simple and computationally efficient. By locally approximating 3D surfaces by planar patches, the 3D model is also suited for analytic surfaces, or surfaces which are specified by an array of surface normal directions at different points on the surface. The basic modelling concepts are also used in extracting shape information from texture. Shape parameters estimation is posed as a maximum likelihood estimation (MLE) problem.

I. Introduction

The inference of the shape of a textured 3D object from its image (or images) has been the concern of many researchers for the past two decades. Shape parameters can be calculated from regular patterns on the surface or from texture gradients. Gibson [1] first proposed the texture density gradient as the primary basis for surface perception by humans. Bajcsy and Lieberman [2] used the two-dimensional Fourier spectrum to detect texture gradient as a cue to depth information.Witkin [3] studied the problem of recovering the local orientation of known 3D surface markings by studying how the marking features are transformed by the projection operation. Davis et al [14 developed an efficient algorithm for recovering local orientations of known 3D surface markings. Ikeuchi [5] also exploited regular patterns on the surface to extract shape information. He used a spherical projection perspective imaging model and studied the local distortions of a repeated texture pattern due to the the image projection. Kender [6] obtained the orientation of a 3D planar surface from the images of parallel edges drawn on it. It relies on an abstract representation (the normalized textural property map) of the effects of surface orientation on a particular texture property, and prestored information about a particular texture pattern. Ohta and his co-workers [7] obtained the a 3D planar surface, by computing a 2D affine transformation which approximates the distortion of the texel patterns under perspective projection. Finally, Brzakovic [8] obtained the orientation for planar surfaces with regular or globally regular directional textures, and perspective camera model. All these cues, no doubt, are essential for surface or object information extraction. A good image model should incorporate all these cues. The emphasis in this paper is on texture cues.

Texture is usually viewed from one of the two prospects, either structural or statistical. In this paper we look at textured images as realizations or samples from parametric probability distributions on the image space. The model that we use is the Gaussian Markov Random Fields (MRF). The reason for that choice is given in section II. The properties of the MRF's and their use in filtering, image modelling and segmentation has been treated in various papers [9-22]. They were shown to be a compact representation for a variety of textures of interest.

The paper is organized as follows. In section II, we introduce the underlying assumptions about the scene and the image formation process. In section III the proposed texture image model is introduced. In IV, we discuss the 3D texture model. Surface recognition discussed in section V. The experiments are presented in section VI.

II. Problem Statement and Assumptions

The goal of this paper is to model images that result from the projective distortions of "homogeneous" textures laid on 3D surfaces, as they are seen by a camera. By a "homogeneous" surface texture we mean a homogeneous texture on a rubber planar sheet (i.e., a 2D homogeneous planar texture) which has been laid down on the surface without any local distortion or folding (see figures 6-7 for examples).

We assume that the surfaces in the scene are mainly Lambertian, i.e., they reflect equally in all directions. Hence, the intensity value of a point on a surface which is viewed from different directions should be the same. Small but noticeable differences between gray-levels recorded in two images would not affect much our results as the textural characteristics of the surface remain essentially unchanged. We assume a camera with either a pin-hole or an orthographic geometry, with its optical-axis parallel to the z-axis, and the image plane parallel to the x-y plane. A viewer centered description for the scene is adopted.

III. 2D Homogeneous Texture Model

For modelling the homogeneous planar texture, we use a Gaussian Markov Random Fields . The reasons for that choice are: (i) they are synthesis models that are capable of producing textures that match and capture amazingly well many man-made as well as natural micro and macro textures [2, 15, 19, 21]; (ii) the parameters (or their associated sufficient statistics) of the model are measurable from data samples and the appropriateness of the model can be assessed objectively by hypothesis testing; (iii) minimum error classifiers are readily built.

III.1 Gaussian Markov Random Field (GMRF) Structure

Let g_{ij} be the intensity at pixel $\mathbf{r} = (i,j)$, g be the image data, and $g_{(\mathbf{r})}$ the data not including the data at point $\mathbf{r}$. The GMRF is described by the following noncausal difference equation

$$g_{\mathbf{r}} = \mu + \sum_{\mathbf{v} \in D_p} \beta_{\mathbf{r}-\mathbf{v}} (g_{\mathbf{v}} - \mu) + n_{\mathbf{r}} \qquad (3.1)$$

where $\beta_{\mathbf{r}-\mathbf{v}} = \beta_{-(\mathbf{r}-\mathbf{v})}$ (which follows from the symmetry property of of the autocorrelation function associated with g, $R_g(m,n) = R_g(-m,-n)$) , and Dp is a neighbor set given by

$$D_p = \{ \mathbf{v} = (k,l) : \| \mathbf{r} - \mathbf{v} \|^2 \le N_p \quad , \text{ and } \mathbf{v} \neq \mathbf{r} \} \qquad (3.2)$$

where p is the order of the process and N_p the maximum square of the distance from point $\mathbf{r}$ to $\mathbf{v}$. $\{n_{\mathbf{r}}\}$ is a Gaussian noise sequence with zero mean and autocorrelation function given by

$$R_n(\mathbf{r},\mathbf{v}) = \begin{cases} \varphi^2 , & \text{if } \mathbf{v} = \mathbf{r} \\ -\varphi^2 \beta_{\mathbf{r}-\mathbf{v}} , & \text{if } \mathbf{v} \in D_p \\ 0 , & \text{otherwise} \end{cases} \qquad (3.3)$$

The joint density function of g is $p(g) \sim \eta(U, \varphi^2 \Psi^{-1})$, where $U = \mu 1$ is the mean vector, and $\varphi^{-2}\Psi$ is the inverse covariance matrix of g. The GMRF is parametrized by a relatively small parameter set $\gamma = (\mu, \varphi^2, \beta)$, with $\beta = (\beta_{10}, \beta_{01}, \beta_{11} , \beta_{1,-1} , ..)$. Under a toroidal lattice approximation $\varphi^{-2}\Psi$ is circulant which implies that $G = DFT(g-U)$ is a white Gaussian field [11-13],

$$p(G) = \prod_{i,j} (1/2\pi N^2 S_{ij})^{1/2} \exp\{-(\sum_{i,j} \| G_{ij} \|^2 / 2N^2 S_{ij})\} \qquad (3.4)$$

where G_{ij} is the ij component of G and $N^2 S_{ij}$ is the power spectral density $N^2 S(\omega_1,\omega_2)$ (or $S(z_1 = e^{\sqrt{-1}\omega_1}, z_2 = e^{\sqrt{-1}\omega_2})$) [9, 11] of the GMRF evaluated at $\omega_1 = 2\pi i/N$, and $\omega_2 = 2\pi j / N$.

$$S(\omega_1,\omega_2) = \varphi^2 / [1 - \sum_{(m,n) \in D_p} \beta_{m,n} \exp\{-\sqrt{-1}(m\omega_1 + n\omega_2)\}] \qquad (3.5)$$

It can be computed anywhere on the unit circles in the z_1-plane and z_2-plane.

IV. 3D Planar Texture Model Structure

In this section we show how to transform the 2D homogeneous GMRF texture model parametrized by γ into a 3D texture model whose structure reflects the foreshortening texture distortions due to the orientation of the plane relative to the camera, and the camera geometry. In particular, we show the functional relationships that exist between the image of a homogeneous textured plane when viewed head-on by a camera, and the image produced by the same plane when it is given an orientation relative to the optical-axis of the camera, for different camera geometry (orthographic and perspective).

IV.1 Planar Surface -- Orthographic Projection Camera Model

Let σ and τ, shown in figure 1, be the slant angle and the tilt angle of the planar surface relative to the viewer coordinate system. If the surface is parallel to the image frame and has no slant or tilt, then the texture in the image

coincides with the texture on the surface.The effects of the slant and tilt of the plane on the image texture under orthographic projection can be easily derived as follows. Consider a textured plane which coincides with the image plane (i.e., the uvw object plane coordinates and the xyz image coordinates coincide, and where the normals to the plane are along w and z). To realize a slant of σ and tilt of τ of the object plane relative to the image plane, we first rotate the object plane by an angle $(\pi/2-\tau)$ about the w-axis. This results into the rotation of the uv axes, with the w-axis remaining the same. We then rotate by an angle of $-\sigma$ the object plane about that new u-axis. Here the vw axes are changing, and the u-axis remains unchanged.These two rotations realize the desired plane slant and tilt, however, the texture on the plane has been rotated by an angle of $(\pi/2-\tau)$. To undo this effect, we rotate the object plane about the new w-axis by an angle $(\tau-\pi/2)$. The rotations are shown in figure 1.

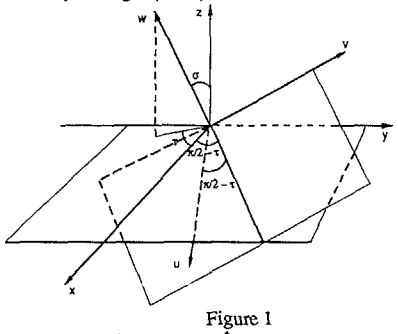

Figure 1

A point with coordinates $(u\ v\ 0)^t$ relative to the uvw coordinates system will have its xyz coordinates given by

$$\begin{bmatrix} x \\ y \\ z \end{bmatrix} = \begin{bmatrix} \sin\tau & \cos\tau & 0 \\ -\cos\tau & \sin\tau & 0 \\ 0 & 0 & 1 \end{bmatrix} \begin{bmatrix} 1 & 0 & 0 \\ 0 & \cos\sigma & \sin\sigma \\ 0 & -\sin\sigma & \cos\sigma \end{bmatrix} \begin{bmatrix} \sin\tau & -\cos\tau & 0 \\ \cos\tau & \sin\tau & 0 \\ 0 & 0 & 1 \end{bmatrix} \begin{bmatrix} u \\ v \\ 0 \end{bmatrix} \tag{4.1}$$

As the point on the object plane is orthographically projected on the image plane, its image coordinates $(i\ j)^t$ are simply $(x\ y)^t$ which are given in (4.1). Hence,

$$\begin{bmatrix} i \\ j \end{bmatrix} = [T] \begin{bmatrix} u \\ v \end{bmatrix} = \begin{bmatrix} 1-\rho\cos^2\tau & \rho\sin\tau\cos\tau \\ \rho\sin\tau\cos\tau & 1-\rho\sin^2\tau \end{bmatrix} \begin{bmatrix} u \\ v \end{bmatrix} \tag{4.2}$$

where $\rho = (1-\cos\sigma)$. (4.2) is also reported in [25].

The effects of the orthographic projection is a scaling (compression) by $\cos\sigma$ of the texture in the direction normal to the rotation axis determined by τ (see figure), i.e., the texture appears uniformly compressed by $\cos\sigma$ in the direction normal to the rotation axis determined by τ. Because of the linearity of the transform in (4.2), the resulting texture is homogeneous.

IV.2 Likelihood Function for the Texture Data on the Slanted and Tilted Plane

Let g_o be the image data of a homogeneous textured plane when viewed head-on. g_o be modelled by a GMRF, with parameter set $\boldsymbol{\gamma}$. The probability distribution function of g_o is $p(g_o \mid \boldsymbol{\gamma})$ and is given in section III. Let g_I be the image data of the same plane when the plane is slanted, and tilted (σ, τ) with respect to the viewer. g_I is a distorted version of g_o, and should be parametrized by $\boldsymbol{\gamma}$, as well as σ, τ.

For a texture on a plane with some slant angle σ and tilt angle τ, a point $r^t = (x\ y\ z)^t = (u\ v\ 0)^t$ on the plane maps orthographically onto the image plane according to the linear transform in (4.2). Since a linear transform (scaling) in the spatial domain correspond to a scaling (linear transform) in the frequency domain, that implies that under the projection model, the power spectral density associated with the texture image on the slanted and tilted plane is

$$S^I_f = [\det[T]]^2\, S^o_{f_o} = [\det[T]]^2\, S^o_{[T]\,f} \tag{4.3}$$

with

$$f_o = [T]\,f, \text{ and } f^t = (i\ j)^t. \tag{4.4}$$

and where $S^o_{f_o}$ is given in (3.5) with $\omega = (2\pi/N)\,f_o$ This can be seen as follows. Let $g_I(r_I)$ be the image intensity of the point $r_I^t = (i\ j)^t$ on the image plane, and let $g_o(r_o)$ be the image intensity of the point $r_o^t = (u\ v)^t$ on the object plane (when viewed head-on). Then, if $r_I = [T]r_o$ (and hence $r_o = [T]^{-1}r_I$), it follows from the Lambertian reflection assumption that

$$g_I(r_I) = g_o(r_o) = g_o([T]^{-1}r_I) \tag{4.5}$$

Taking Fourier transform yields

$$G_I(f) = G_o(f_o) = \det[T]\, G_o([T]\,f) \tag{4.6}$$

Squaring (4.6) and taking expectation yields the result in (4.3).

The likelihood function (under a torus structure) of the DFT of the image data g_I is given by

$$p(g_I) = p(G_I|\boldsymbol{\gamma},\sigma,\tau) = \prod_f (2\pi N^2 S^I_f)^{-1/2} \exp\{-(\Sigma_f |G_f|^2/(2N^2 S^I_f)\} \tag{4.7}$$

where S^I_f is given in (4.3).

Note that no interpolation is needed to compute $S^o_{[T]f}$, as the power spectral can be computed anywhere on the unit circles in the z_1-plane and z_2-plane as explained in section III.

IV.3 Perspective Projection Camera Model

The orthographic camera geometry model is a good approximation to the perspective projection model as long as the scene depth is small relative to the average distance from the camera. Since the perspective projection of a point on the planar surface depends on its depth relative to the image frame coordinate system. The transformations in (4.2) are now nonlinear and according to [23]

$$i = (f / f\text{-}z)\ u \tag{4.8}$$

$$j = (f / f\text{-}z)\ v \tag{4.9}$$

where f is the focal length of the camera, and z is the depth of the point $(i\ j\ z)^t$ on the slanted and tilted plane. z is a known function if i, j, σ and τ. The result of the transformations in (4.8) and (4.9) is a nonhomogeneous planar texture which can not be modelled by a homogeneous GMRF.

IV.3.1 Affine Transform Approximation To Perspective Projection

To overcome the problem of the non-homogeneity of the planar texture under perspective projection, we approximate the perspective projection by the affine transformation due to Ohta et al [7], and used in Brown's et al [25]. The result of the approximation (as shown shortly) is that within a local patch a point on the object plane maps onto the image point according to a linear transform, and hence a locally homogeneous texture patch in the image plane (as discussed in IV.2). The non-homogeneous texture is approximated by piecewise homogeneous ones. For a relatively small patch on the plane, this results in a very accurate approximation to the perspective projection.

The projection is shown in figure 2, for a point P (on the object plane) which is part of a local patch on the plane whose centroid has βA, βB, and $-\beta$, as the x, y, and z coordinates respectively. P has coordinates $(x\ y\ z)^t$ with respect to O, and $(u\ v\ 0)^t$ with respect to uvw coordinate frame centered at O". P is first projected onto the plane which intersects the object plane at point O", and which is parallel to the image plane. The projection is along the O O'O" line. This projection approximately mimics the skewing effects associated with the perspective projection. The projected point P_1 on the β-plane has coordinates $(x_1\ y_1\ -\beta)^t$ with respect to O. P_1 is perspectively projected on the image plane onto the point P_2, whose coordinates are $(x_2\ y_2\ -f)^t$ with respect to O, and $(i\ j\ 0)^t$ with respect to O'.

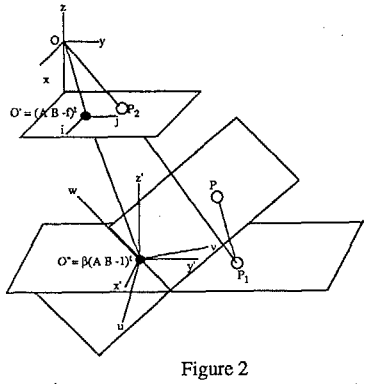

Figure 2

A point $(u\ v)^t$ on the object plane $(-z = px + qy + d)$ maps onto an image point $(i\ j)^t$ according to the linear transform

$$\begin{bmatrix} i \\ j \end{bmatrix} = [T] \begin{bmatrix} u \\ v \end{bmatrix} = \frac{1}{\beta} \begin{bmatrix} 1-Ap & -Aq \\ -Bp & 1-Bq \end{bmatrix} \begin{bmatrix} 1-\rho\cos^2\tau & \rho\sin\tau\cos\tau \\ \rho\sin\tau\cos\tau & 1-\rho\sin^2\tau \end{bmatrix} \begin{bmatrix} u \\ v \end{bmatrix} \tag{4.10}$$

where p and q are given

$$p = \tan\sigma\cos\tau \tag{4.11}$$

$$q = \tan\sigma\sin\tau \tag{4.12}$$

and β equals to

$$\beta = \frac{d}{f(1-Ap-Bq)} \tag{4.13}$$

Finally, note that A and B in (4.10) are related to the image centroid coordinates of the patch A_I, and B_I as follows

$$A = (s\,A_I)/N$$

$$B = (s\,B_I)/N \tag{4.14}$$

where s is ratio of the side of the image frame relative the distance of the focal point to the image frame of the camera, i.e.,

$$s = N / f \tag{4.15}$$

Realistic values of s would be 1/2 or 1/4.

The likelihood function of an nxn square image data patch with centroid (A,B) is given in (4.7) but with the matrix [T] given in (4.10), and with the (i,j) coordinates expressed relative to the center (A,B). The joint likelihood function for the whole NxN image texture is approximated by

$$p(g_I) \approx \prod_k p(G_k|\boldsymbol{\gamma},\sigma,\tau,A_k,B_k) \tag{4.16}$$

where G_k is the DFT of an nxn image data patch with centroid (A_k, B_k).

Remarks : (i) The transform in (4.10) is different than the one reported in Ohta's and Brown's papers. It is a point by point mapping that results in having the object coordinates and the image coordinates coinciding if the slant and tilt were undone. The determinant of the transformation matrix in (4.10) and in Ohta's paper are one and the same for f = -1; (ii) When the window centroid is collinear with the camera axis (i.e., A = B = 0, the transform in (4.10) is the same as for the orthographic projection transform given in (4.2) if the $(1/\beta)$ factor is discarded.

IV.4 Maximum Likelihood Estimation (MLE) for the Slant and Tilt

When γ is known, the MLE for σ and τ are obtained by maximizing (4.7) (for orthographic camera model) or (4.16) (for perspective camera model) with respect to σ and τ. When γ is not known apriori, then the problem becomes unidentifiable, and neither the original texture nor σ and τ can be recovered just from the projective relation. Any value of σ and τ defines a possible surface orientation and a possible reconstruction of the unprojected texture. That means that there will be a family of possible texture/orientation pairs $\{(T_1,O_1), (T_2,O_2),..., (T_n,O_n)\}$ that can generate the image texture T (see figure 3). The projection can be thought of as many-to-one mapping.

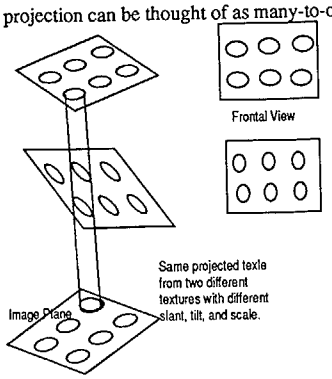

Figure 3

V. Generalization to More Complex Regular Surfaces

By locally approximating 3D surfaces by planar patches, the 3D planar texture model is also suited for analytic surfaces, or surfaces which are specified by an array of surface normal directions at different points on the surface. The image data is partitioned into nonoverlapping square windows which are assumed to emanate from locally planar patches. For each such window, the plane orientation parameters are computed as explained in section IV. The resulting texture is a 3D surface texture model. In this paper we concentrate on the subclass of quadric surfaces, namely, plane, cylinder, and sphere, and show how to classify a given image patch into one of these surfaces, which are assumed to have the same "homogeneous" texture (see figures 6-7).

V.1 Surface Patch Classification from Surface Normals -- Known Texture Case

The problem here is to classify a given surface patch into one the three surfaces from a set of computed unit normals N_k's. There are many ways of classifying an image patch based on the unit normals (see for example [26]). In this paper we elected to use a least square method, where it has been assumed that the σ and τ components of the unit normal N (whose coordinates in spherical space are $(1\ \sigma\ \tau) = (1\ \mathbf{n})$), have white Gaussian perturbation which are independent of each other, i.e.,

$$\sigma(x,y) = \sigma(x,y) + w_1(x,y) \quad (5.1)$$

$$\tau(x,y) = \tau(x,y) + w_2(x,y) \quad (5.2)$$

where

$$w_c(x,y) \sim \eta(0,\psi^2),\ c = 1, 2 \quad (5.3)$$

$\sigma_k(x_k,y_k)$ and $\tau_k(x_k,y_k)$ are the true surface slant and tilt, respectively, evaluated at the window's center (x_k,y_k). $n_k = \{\sigma_k(x_k,y_k),\tau_k(x_k,y_k)\}$ is a function of the parameters of the underlying surface. Its equation can be derived in a straight forward manner from the equations of a plane, cylinder, or sphere. If the parameters of the surface are not known beforehand, we can estimate them from the given $\mathbf{n_k}$'s.

The surface patch is classified as "plane" (P), "cylinder" (C), or "sphere" (S) using the decision rule

$$\text{class} = \arg[\max_{\omega \in \{P,C,S\}} p(\mathbf{n} \mid \varphi_\omega^*, \omega)] \quad (5.4)$$

where $\mathbf{n} = (\mathbf{n_1}, \mathbf{n_2},..., \mathbf{n_M})$, and φ_ω^* is the maximum likelihood estimate (MLE) of the surface parameters under the assumption that the surface type is ω.

IV.2 Surface Patch Classification -- Unknown Texture Case

As in the case of a single planar surface, the surface true orientation of the planar facets that constitute the surface can't be recovered uniquely when the textured model parameters γ of the homogeneous rubber sheet are unknown apriori. Despite that, we are still able to recognize the surface type (e.g., plane, cylinder, or sphere), and estimate the radius (of sphere and cylinder). For a given surface patch within an M-window neighborhood, we consider the data in any of the window (say window m), and obtain the pair (T*,O*) that will best fit the data in that window by maximizing the likelihood function with respect to $T = \gamma$, $O = (\sigma, \tau)$

$$\max_{\gamma,\sigma,\tau} p(g_m \mid \gamma, \sigma, \tau) \quad (5.5)$$

where g_m is the data in the mth window. Let $T^* = \gamma^*$, and $O_m^* = (\sigma_m^*, \tau_m^*)$. Suppose the real texture/orientation pair were $T_t = \gamma_t$, and $O_{mt} = (\sigma_{mt}, \tau_{mt})$, then the use of the wrong texture has introduced an offset $O_{off} = (\sigma_{off},\tau_{off})$, i.e.,

$$O_{mt} = O_m^* + O_{off} \quad (5.6)$$

For any window k (g_k) in the M-window neighborhood image patch, we compute the MLE for O_k,while imposing the T* texture model

$$\max_{O_k} p(g_k \mid T^*, O_k) \quad (5.7)$$

Because the imposed texture is not the true one, the estimated orientation O_k^* is offset from the true O_{kt} by O_{off}. Despite, the offset, the relative orientation of the windows are invariant to the use of the wrong texture. That is to say

$$O_{mt} - O_{kt} = O_m^* - O_k^* \quad (5.8)$$

Hence, we can recognize the surface type by exploiting the relative orientation of the windows associated with the image patch. For a plane, all the local facets will have the same orientation O (although it might not be the true one). For a cylinder, the facets will exhibit a symmetry with respect to an axis. For a sphere, the facets will exhibit a symmetry with respect to a point.

VI. EXPERIMENTS

In the first part of the section, we show the goodness of the 3D texture model in capturing the texture distortions. Figure 4 shows the effects of slant ant tilt on a planar texture under orthographic and perspective projection, respectively. Figure 4b shows a synthesized frontal view of the homogeneous "raffia" texture shown in figure 4a. The GMRF parameters were estimated from a 64x64 data window of the image shown in figure 4a. Using the estimated parameters from figure 4a, and using the transform in section IV.1, figure 4c shows the orthographic projection of the texture when the plane has a slant of 60°, and a tilt of 0°. As expected the generated field underwent a compression in the direction which is perpendicular to the line that sustains a 0° angle with the x-axis (i.e., the y-axis). In figure 4d, we shows the orthographic projection of the texture when the plane has a slant of 60°, and a tilt of 45°. As expected the generated field underwent a compression in the direction which is perpendicular to the line that sustains a 45°. In figure 4e, we show the texture under perspective projection when the plane has a slant of 60° and a tilt of 0°, and using the linear transformation in section IV.3.1. In figure 4f, we show the perspective distortion of the texture in figure 4a, when the plane undergoes a slant of 60° and a tilt of 45°. It is interesting to note that the depth effect due to the plane going away from the viewer is quite noticeable. In figure 5c, we show the perspective projection of the "water" texture shown in figure 5a (whose synthesized frontal view is shown in figure 5b) when the plane undergoes a slant of 60° and a tilt of 0°. It is interesting to note that unlike the raffia texture, the water texture does not have a strong directionality, and hence the convergence of the lines towards the horizon phenomenon that is observed in the raffia case, is absent here. Nonetheless, the blurring and fading away of the texture as we move away from the observer is quite noticeable. In figures 6-7, we show the rendering of the texture on different surfaces under orthographic and perspective projections. In figure 6a, and 6b, we show the raffia texture rendered on a sphere of radius 100 pixels, and which is about 200 pixels (in the z-direction) away from the viewer. In figures 7a and 7b, the simulations in figure 6, are repeated for a nail object that consists of a cylinder whose axis is parallel to the y-axis, and a sphere.

The second part deals with the shape from texture extraction problem. We ran experiments on the real surfaces shown in figure 8 These were : (a) a cylinder covered with grass texture; (b) a cylinder covered with paper texture; (c) a plane covered with paper texture; and (d) a sphere covered with fabric texture. The classification of an image surface patch for cases (a) - (c) were in favor of the correct surface; and the distribution of the estimated slant and tilt in the different windows were consistent with the expected ones. For case (d), the classification was again in favor of a sphere, but the estimated slant and tilts in some of the windows were not consistent with the expected ones. The main reason behind that was that the fabric has been laid on the sphere by hand, resulting in folding, stretching, and distortion. Consequently, the image textures in some of the windows were not consistent with how they should appear if they emanated from patches on a spherical surface.

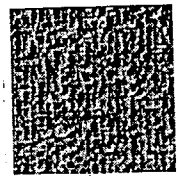

Original texture
(a)

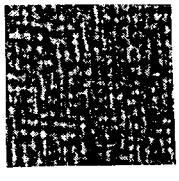

Synthesized texture -- Frontal View
(b)

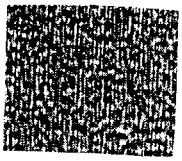

Orthographic Projection σ=60°,τ=0°
(c)

Orthographic Projection σ=60°,τ=45°
(d)

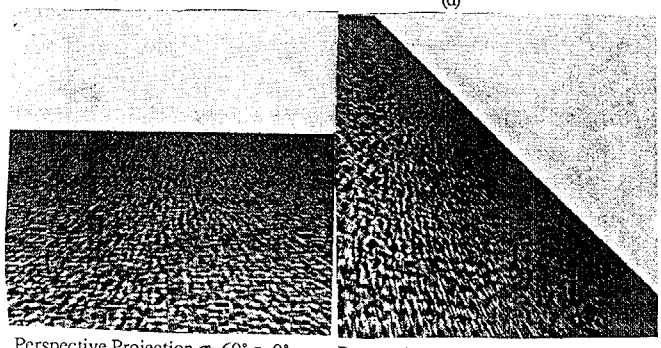

Perspective Projection σ=60°,τ=0°
(e)

Perspective Projection σ=60°,τ=45°
(f)

Planar Surface with "Raffia" Texture
Figure 4

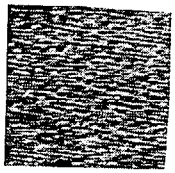

Original texture
(a)

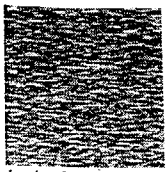

Synthesized texture -- Frontal View
(b)

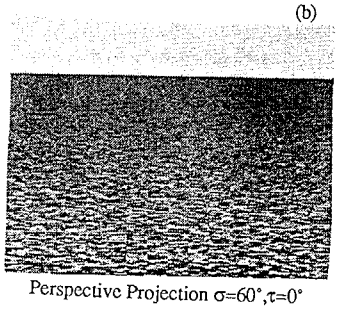

Perspective Projection σ=60°,τ=0°
(c)

Planar Surface with "Water" Texture
Figure 5

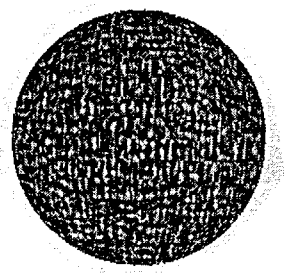

(a) Orthographic Projection

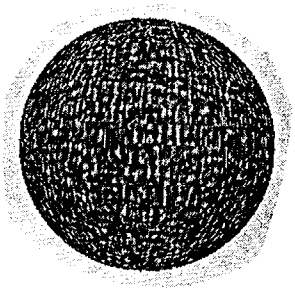

(b) Perspective Projection

Sphere
Figure 6

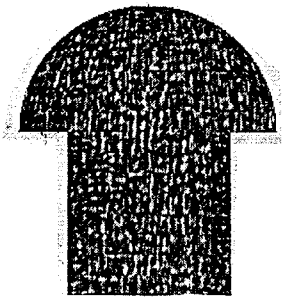

(a) Orthographic Projection

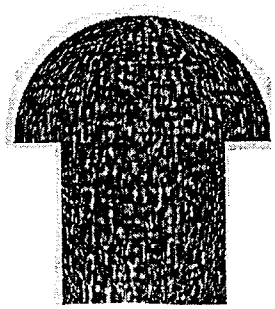

(b) Perspective Projection

Nail
Figure 7

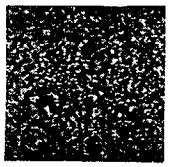

(a)

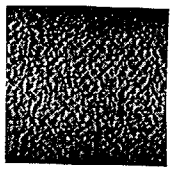

(b)

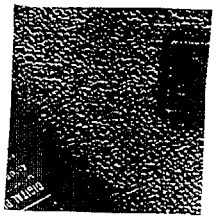

(c)

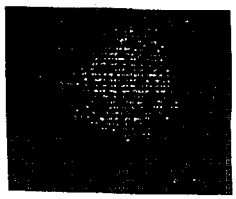

(d)

Figure 8

REFERENCES

[1]. J.J. Gibson, The Perception of the Visual World, Houghton Mifflin Co., Boston 1950.

[2]. R. Bajcsy and L. Lieberman, " Texture Gradients as a Depth Cue," Comp. Graphics and Image Processing 5, 1976.

[3]. A. P. Witkin, " Recovering surface Shape and Orientation from Texture," Artificial Intelligence, Vol. 17, 1981.

[4]. L. S. Davis, L. Lanos, and S. M. Dunn, "Efficient Recovery of Shape from Texture," IEEE Trans. on PAMI, Vol. 5 No. 5, 1983.

[5]. K. Ikeuchi, "Shape from Regular Patterns," Artificial Intelligence, Vol. 22, 1984.

[6]. J. R. Kender, " Shape from Texture : A Computational Paradigm," Proc. of the Image Understanding Workshop, May 1979.

[7]. Y. Ohta, K. Maenobu, and T. Sakai, " Obtaining Surface Orientation from Textels under Perspective Projection," Proc., IJCAI, 1980.

[8]. D. Brzakovic, Computer Based 3D Description from Texture, Ph. D. dissertation, Department of Electrical Engineering, University of Florida, 1984.

[9]. J. Woods," Two-Dimensional Discrete Markov Random Fields," IEEE Trans. Inf. Theory, vol. IT-18, 1972.

[10]. J. Besag, "Spatial Interaction & the Statistical Analysis of Lattice Systems," Journal of the Royal Statistical Society, Series B, 36, 1974.

[11]. J. Besag and P. Moran, "On the Estimation and Testing of Spatial Interaction in Gaussian Lattices," Biometrika, Vol. 62, 1975.

[12]. R. Kashyap and R. Chelappa, "Estimation and Choice of Neighbors in Spatial Interaction Models of Images," IEEE Trans. Information Theory, Jan. 1983.

[13]. R. Chelappa and R. Kashyap, " Texture Synthesis Using 2D Noncausal Autoregressive Models," IEEE Trans. on Acoustics, Speech, and Signal Processing, Vol. ASSP-33, Feb. 1985.

[14]. R. Cross & A. Jain," Markov Random Field Texture Models," IEEE on PAMI, vol. 5, 1983.

[15]. F. S. Cohen, *Markov Random Fields for Image Modelling & Analysis* , U. Desai, Ed., Kluwer Academic Press, September 1986.

[16]. S. Geman & D. Geman, "Stochastic Relaxation, Gibbs Distributions & the Bayesian Restoration of Images," IEEE Trans. on PAMI, Vol. PAMI-6, Nov. 1984, pp. 721-741.

[17]. H. Derin & H. Elliot, "Modelling & Segmentation of Noisy & Textured Images Using Gibbs Random Fields," IEEE Trans. on PAMI-9, Jan. 1987.

[18]. R. Cristi, "Multi-Level Image Segmentation by Markov Random Field Models and Kalman Filtering," Intr. Conf. on Acoustics, Speech, and Signal Processing, NY, April 1988.

[19]. F. S. Cohen & D.B. Cooper,"Simple Parallel Hierarchical & Relaxation Algorithms for Segmenting Noncausal Markov Random Fields," IEEE Trans. on PAMI, March 1987.

[20]. Z. Fan & F.S. Cohen, "Textured Image Segmentation as a Multiple-Hypothesis Test," IEEE Trans. on Systems & Circuits, June 1988.

[21]. F.S. Cohen & Z. Fan , " Unsupervised Textured Image Segmentation," Proc. of the Int. Conf. on Intelligent Autonomous Systems, Amsterdam, The Netherlands, Dec. 1986.

[22]. F.S. Cohen & Z. Fan, " Rotation and Scale Invariant Texture Classification," Proc. of the IEEE Conf. on Robotics & Automation, Philadelphia, PA, April 1988.

[23]. A. Rosenfeld and A. Kak, *Digital Picture Processing*, Second Edition, Academic Press, 1982.